2025 IMEKO TC-6 International Conference on
Metrology and Digital Transformation - **M4DConf 2025**
Benevento, Italy, September 3-5, 2025

Automating Photometric Measurements Using LabVIEW-Python-Based AI: Enhancing Precision in Luminous Intensity, Responsivity, Illuminance, and Flux Analysis at Saudi Standards, Metrology, and Quality Organization-SASO-KSA

Mohammad D. AlMelfi, Rawan A. AlMutairi, Fahad A. AlMuhlaki, Saad A. Bin Qoud, Rayan A. AlYousefi, I. AlFaleh, N. Qahtani, A. El-Matarawey

NMCC-SASO- Saudi Arabia

Abstract - **This work explores the automation of a photometry laboratory by integrating LabVIEW as the primary control and data acquisition platform, coupled with a Python-based artificial intelligence (AI) algorithm for intelligent analysis and optimization. The system is designed to measure and analyze critical photometric parameters such as luminous intensity, luminous responsivity, illuminance, and luminous flux—all of which are essential for evaluating the performance of light sources like tungsten halogen lamps, LEDs, displays, and optical sensors. By automating traditionally manual processes, the system enhances both the accuracy and efficiency of photometric testing.**

LabVIEW provides an intuitive graphical interface to control instruments, log data, and visualize results in real time. Meanwhile, the Python AI component improves decision-making by learning from historical data, predicting trends, and detecting anomalies or inconsistencies in measurements. The AI model optimizes calibration routines, reduces human error, and enables adaptive testing scenarios based on environmental conditions or device behavior.

Together, LabVIEW and Python form a powerful, flexible platform that brings modern intelligence to photometry labs, making them faster, smarter, and more reliable. This approach demonstrates how combining industrial automation tools with machine learning can revolutionize traditional optical testing environments, paving the way for advanced lighting technologies and robust quality assurance systems.

Keywords: Python, AI, Algorithms, Automation, Photometry, Responsivity, Illuminance, Flux, SASO, NMCC

I. INTRODUCTION

The field of photometry is essential for evaluating the performance of light sources such as tungsten halogen lamps, LEDs, displays, and optical sensors. Key parameters like luminous intensity [1], luminous responsivity [2], illuminance [3], and luminous flux [4] are crucial for characterizing these devices. Traditionally, photometric testing has relied on manual processes, which are not only prone to human error but also time-consuming and often lack adaptability to dynamic testing conditions.

This paper introduces an innovative solution to automate a photometry laboratory by integrating LabVIEW as the primary control and data acquisition platform with a Python-based artificial intelligence (AI) algorithm for advanced analysis and optimization using a powerful integrated library [5-12]. The system automates conventional manual tasks while introducing intelligent features such as predictive analytics, anomaly detection, and adaptive testing scenarios. This combination significantly enhances the accuracy, efficiency, and reliability of photometric measurements, transforming the way photometry labs operate. The SASO-NMCC photometry lab comprises various facilities and equipment that rely on custom software for operation. Recently, the lab faced challenges due to software failures that caused damage to certain light sources. The issue stemmed from the inability of the software to regulate the electric current passing through the lamps, resulting in currents exceeding critical thresholds. To address this problem, the digital transformation team conducted a thorough analysis and proposed replacing the outdated software with a new model. This updated system combines two powerful programming languages: LabVIEW for automation and fractional Proportional Integtration (PI control) algorithm and Python for data analysis, integrated into an interactive AI-driven graphical user interface platform.

II. EQUIPMENT AND SYSYTEM SETUP

Table 1 provides a detailed overview of each piece of equipment utilized in the laboratory, outlining its purpose, functionality, and relevance to photometry and electrical measurements. The information is systematically organized by equipment type, manufacturer, model, serial number, and a provided description for clarity and ease of reference.

Table1. Photometry lab equipment

Equipment	Manufacturer	Model	Serial Number
Digital Multimeter	Agilent Keysight	3458A	MY45050860
Digital Multimeter	Agilent Keysight	3458A	MY45050862
Photocurrent Meter	PRC Krochmann	Radiometer/ Photometer 211	141118-20
Shunt Resistance	Guildline Instruments	9230A-15R	71630
DC Power Supply	Heinzinger electronic GmbH	PTN 250-20	3449 10675
Current Source	Keithley	6220	4056589
Picoammeter	Keysight	B2981A	--

<u>Digital Multimeter</u> A high-precision device designed to measure electrical parameters such as voltage, current, and resistance. It plays a critical role in photometric testing by monitoring the voltage applied to light sources, ensuring stable power delivery during experiments. This stability is essential for accurate photometric calculations, as fluctuations in voltage can impact the performance of light sources. By tracking supply voltage and current, the multimeter provides an indication of the consistency and reliability of the electrical input to photometric devices.

<u>Photocurrent Meter</u> A specialized instrument used to measure the photocurrent generated by Photometer heads, which are photodiodes with $V(\lambda)$ mosaic filter, when exposed to light. Equipped with a thermoelectric cooler, it maintains a constant temperature for the photodiode, ensuring stable and precise measurements. This device is instrumental in calculating responsivity by comparing the incident optical power to the measured photocurrent. It is also used to determine the responsivity of devices under test, making it a vital tool for evaluating detector performance.

<u>Shunt Resistance</u> A precision resistor, typically with a low value (in milliohms) and tight tolerance, used to measure currents by converting them into measurable voltage drops across the resistor. Shunt resistors are commonly employed in current-sensing applications where direct current measurement is impractical. In photometric testing, they are used to measure the current drawn by light sources, providing critical data for analyzing device behavior under various operating conditions.

<u>DC Power Supply</u> A stable and adjustable direct current (DC) power source that supplies power to electronic devices. Known for its high stability and low ripple, this power supply ensures consistent operating conditions during photometric testing. It provides a constant voltage or current output within specified limits, making it ideal for powering light sources such as tungsten halogen lamps and LEDs. This equipment is essential for characterizing the electrical behavior of devices under different power levels and ensuring reliable test results.

<u>Current Source</u> A highly stable and precise instrument used to deliver a controlled amount of current to a device under test. In photometric applications, it drives light sources, such as tungsten halogen lamps and LEDs, at specific current levels to evaluate their performance under controlled conditions. This capability is crucial for testing luminous intensity and luminous flux as a function of current, enabling detailed analysis of device characteristics.

<u>Picoammeter</u> An ultra-sensitive instrument capable of detecting extremely small currents, typically in the picoampere range. It is used to measure dark current or leakage current in photodetectors and optical sensors, which is critical for characterizing device sensitivity and noise performance under low-light conditions. The picoammeter's precision makes it indispensable for advanced research and development in photometry.

Together, these instruments form a comprehensive setup for photometric testing. The Digital Multimeter and Current Source ensure accurate electrical characterization, while the Photocurrent Meter and Picoammeter enable precise optical measurements. The Shunt Resistance and DC Power Supply provide the necessary tools for controlling and stabilizing the testing environment. This combination supports a wide range of applications in photometry, from fundamental measurements to advanced research and development, as illustrated in Figure 1.

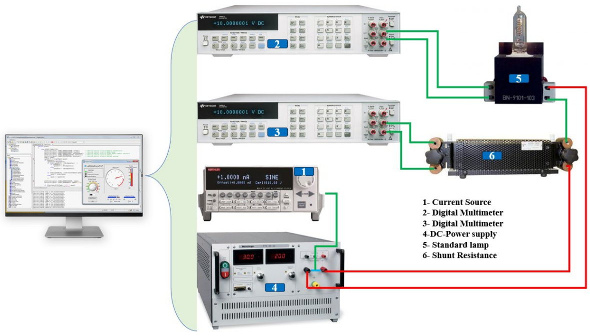

Fig 1. Photometry lab equipment

The diagram 2 and figure 3 illustrate a photometric measurement setup, which is used in laboratory for characterizing light sources and optical devices.

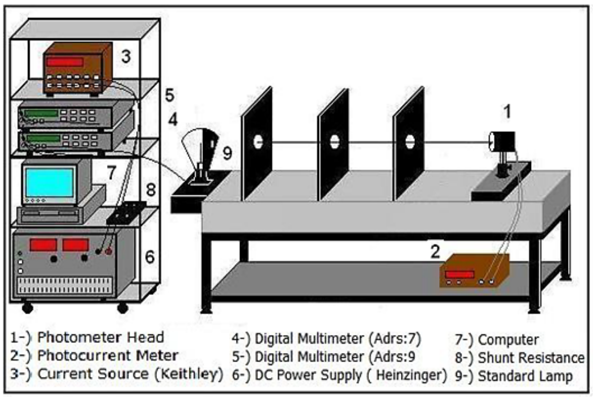

Fig 2. Photometric Measurement setup

Fig 3. Photometric Measurement Equipment

The Photometer Head serves as the sensor component responsible for measuring the intensity or flux of visible light emitted by a source. It captures incoming light and converts it into an electrical signal proportional to the light intensity, which is then connected to the Photocurrent Meter (2) or Picoammeter for further analysis. The Light Source is powered by the DC Power Supply (6) and driven by the Current Source (3) to ensure precise control over its operation. The output of the light source is measured using the Photometer Head (1) and the Photocurrent Meter (2). For calibration purposes, a Standard Lamp (9) is included in the setup. This lamp provides a known light output, enabling accurate calibration of the Photometer Head (1) and ensuring reliable measurement results. At the core of the system, the computer (7) acts as the central hub, controlling the Current Source (3), monitoring real-time measurements, and analyzing collected data. This versatile setup can be adapted for various photometric measurements, including luminous intensity, illuminance, and luminous responsivity of photometers.

III. PROGRAMMING DESIGN

The proposed automation framework is built on two core components: LabVIEW and Python AI. LabVIEW acts as the foundation for instrument control, real-time data acquisition, and visualization, while Python handles advanced data processing through machine learning algorithms. This integration creates a seamless workflow that combines hardware control with intelligent software capabilities.

1. LabVIEW for Instrumentation and Data Acquisition

LabVIEW, developed by National Instruments, offers a graphical programming environment that simplifies the creation of complex measurement systems. In this setup, LabVIEW serves as the central tool for instrument control, interfacing with photometric instruments via standard communication protocols such as GPIB, USB, and Ethernet. It logs measurement data in real time and stores it in structured formats for further analysis. Additionally, its user-friendly graphical interface enables operators to monitor test progress, view live results, and generate reports, as shown in figures 4 and 5. The LabVIEW workflow includes the following key steps:

a) Initialization: All connected instruments are initialized and configured for testing.
b) Data Acquisition: Measurements are taken at predefined intervals and logged into a database.
c) Real-Time Visualization: Results are displayed on a dashboard, allowing operators to monitor the testing process in real time.
d) Exporting Data: Collected data is exported to a CSV file for further analysis by the Python AI component.

This structured approach ensures efficient data collection, real-time monitoring, and seamless integration with the Python-based intelligent processing system.

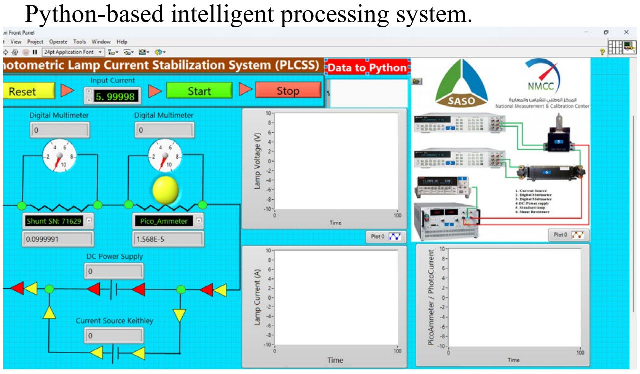

Fig 4. Controlled front panel

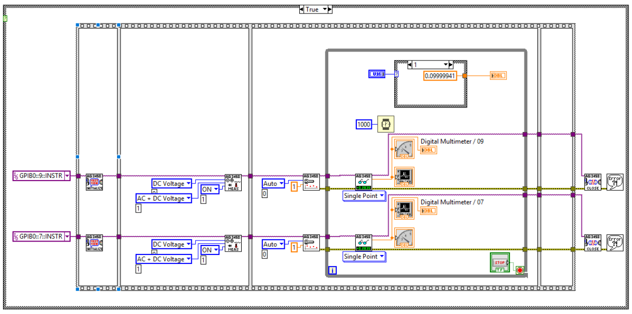

Fig 5. Piece of block diagram related to the automation of multimeters

2. Python AI for Smart Analysis and Optimization

The Python AI component utilizes powerful libraries such as TensorFlow, Scikit-learn, and Pandas to implement advanced machine learning models. These models analyze historical data to predict future trends in photometric parameters, enabling proactive decision-making. Additionally, the AI detects outliers or inconsistencies in measurements, flagging potential issues in the testing process. Adaptive algorithms further enhance the system by optimizing calibration routines and adjusting testing parameters based on environmental conditions or device behavior. Python Workflow includes the following steps:

a) Data Preprocessing: Raw data collected from LabVIEW is cleaned, normalized, and prepared for analysis [13, 14].
b) Model Training: Machine learning models are trained using both live and historical datasets to ensure accurate and reliable predictions.
c) Prediction and Optimization: The trained models dynamically forecast trends in measurement parameters, enabling real-time optimization of testing processes.
d) Hyperparameter Tuning: Parameters generated by the AI are fed back into the LabVIEW system to refine and improve the accuracy of future tests [15, 16].

This workflow ensures that the system continuously learns and adapts, enhancing the precision and efficiency of photometric testing through intelligent analysis and optimization.

The AI component adds a layer of intelligence to the system, enabling it to learn from past data and make informed decisions about future tests related to percentage of current generated by DC power supply and precision current by Keithley. The system adapts to changing conditions, such as variations in ambient light or temperature, ensuring consistent performance across different environments. The modular design of the system allows for easy integration of additional instruments or upgrades to the AI algorithms. While implementing the system, several challenges were encountered. Data synchronization is ensuring seamless communication between LabVIEW and Python, it is required a careful configuration of data exchange protocols [17-22].

IV. MODEL ARCHITECTURE

The flowchart in figure 6 outlines a typical machine learning and data analysis pipeline, the model architecture is described according to series of equations and expressions.

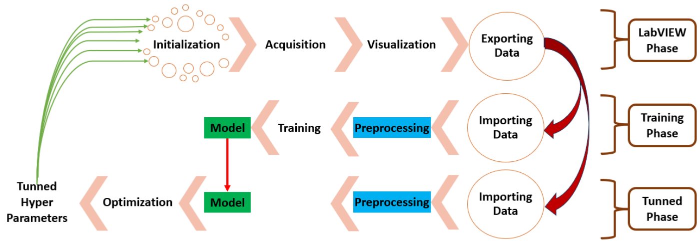

Fig 6. Model architecture and data pipeline

1. *Initialization*, this step involves setting up the environment and defining initial parameters.

$$Initialization: \boldsymbol{\mathcal{P}} = \{\boldsymbol{\theta_o}, \boldsymbol{\varphi_o}, \boldsymbol{w_o}, \ldots\} \quad 1$$

where $\boldsymbol{\mathcal{P}}$ represents the set of initial parameters, and $\boldsymbol{\theta_o}, \boldsymbol{\varphi_o}, \boldsymbol{w_o}$ are initial hyperparameters then model parameters.

2. *Acquisition*, data collected from automated equipment.

$$Acquisition: \boldsymbol{\mathfrak{D}_{raw}} = \{\boldsymbol{x_1}, \boldsymbol{x_2}, \boldsymbol{x_3}, \ldots\} \quad 2$$

where $\boldsymbol{\mathfrak{D}_{raw}}$ is the raw dataset consisting of n samples.

3. *Exporting Data,* data stored and exported in csv files to processed and analyzed for further use.

$$Exporting: \boldsymbol{\mathcal{D}}_{exported} = \boldsymbol{\mathcal{D}}_{processed} \quad 3$$

4. *Importing Data (Training Phase),* Data is imported into the training phase for preprocessing and modelling.

$$\text{Importing (Training)}: \boldsymbol{\mathcal{D}}_{imported} = \boldsymbol{\mathcal{D}}_{processed} \quad 4$$

5. *Preprocessing*, Raw data is cleaned, normalized, and transformed.

$$\text{Preprocessing}: \boldsymbol{\mathcal{D}}_{processed} = \boldsymbol{P}(\boldsymbol{\mathcal{D}}_{raw}) \quad 5$$

6. *Preprocessing*, model is trained using the preprocesses data.

$$\text{Training}: \boldsymbol{\mathcal{M}} = \boldsymbol{T}\left(\boldsymbol{\mathcal{D}}_{processed}, \boldsymbol{\theta}\right) \quad 6$$

where $\boldsymbol{\mathcal{M}}$ is the trained model, $T(\cdot)$ is the training function, and θ are the model parameters.

7. *Optimization*, hyperparameters are tuned to optimize the model's performance.

$$\text{Optimization}: \boldsymbol{\theta}^* = \boldsymbol{O}(\boldsymbol{\mathcal{M}}, \boldsymbol{\mathcal{D}}_{\text{validation}}) \quad 7$$

where θ^* are the optimized hyperparameters, $O(\cdot)$ is the optimization function, and $\boldsymbol{\mathcal{D}}_{\text{validation}}$ is the validation dataset.

8. *Preprocessing (Tuned Phase),* Data is preprocessed again with updated techniques based on insights from the training phase.

$$\text{Preprocessing (Tuned)}: \boldsymbol{\mathcal{D}}_{\text{tuned}} = \boldsymbol{P}'(\boldsymbol{\mathcal{D}}_{\text{raw}}) \quad 8$$

where $P'(\cdot)$ is an updated preprocessing function.

9. *Importing Data (Tuned Phase),* tuned data is imported for further processing and deployment.

$$\text{Importing (Tuned)}: \boldsymbol{\mathcal{D}}_{\text{imported\_tuned}} = \boldsymbol{\mathcal{D}}_{\text{tuned}} \quad 8$$

10. *Model (Tuned Phase),* The final model is deployed and used for inference.

$$\text{Tuned Model}: \boldsymbol{\mathcal{M}}_{\text{final}} = \boldsymbol{\mathcal{M}}(\boldsymbol{\theta}^*) \quad 9$$

V. RESULTS AND DISCUSSION

Table 2 summarize the average of eight runs measurements for ten lamps, that indicates perfect match with traceable nominal values from calibration certificates.

Table 2. Ten validations of software with Lamp nominal values

Meas. No.	Lamp Serial No.	Lamp Certificate current Input current	Lamp Certificate Voltage	Lamp Measured Current	Lamp Measured Voltage 07	Current Power supply	Precession current source	Shunt voltage	Shunt Resistance	Calculated current	Delta V	Delta I	% supply	% PCS	Stopwatch (Power supply)
1	1009	5.892	30.835	5.892	31.117	5.85	0.03882	0.58919	0.0999941	5.89224764	0.282	0.00024764	99.287169	0.65885947	-
2	1115	5.916	30.939	5.91601	31.18259	5.87	0.03863	0.5915929	0.0999941	5.91627806	0.24359	0.00027806	99.2222799	0.65297388	-
3	1097	5.962	31.291	5.96194	31.60531	5.91	0.0405	0.5961906	0.0999941	5.96225777	0.31431	0.00025777	99.1288071	0.67930908	-
4	A	4		3.99999	30.42339	3.95	0.04112	0.3999972	0.0999941	4.00020801		0.00020801	98.7502469	1.02800257	-
5	B	6		6.00003	62.83999	5.95	0.03919	0.6000021	0.0999941	6.00037502		0.00037502	99.1661708	0.6531634	-
6	C	5		4.99959	45.26392	4.95	0.04345	0.5000256	0.0999941	5.00055103		0.00055103	99.0081187	0.86907126	01:28.6
7	D	7.246	86.08	7.24599	88.30552	7.2	0.03799	0.724591	0.0999941	7.24633753	2.22552	0.00033753	99.3653041	0.52428999	01:28.1
8	1088	5.898	30.548	5.89799	30.51875	5.85	0.03974	0.5897976	0.0999941	5.898324	-0.02925	0.000324	99.186333	0.67378887	01:28.5
9	1076	5.93	30.548	5.93001	30.88055	5.88	0.03774	0.5930004	0.0999941	5.93035389	0.33255	0.00035389	99.1566625	0.63642388	01:28.1
10	1090	5.908	30.705	5.908	30.65335	5.86	0.04023	0.5907978	0.0999941	5.90832659	-0.05165	0.00032659	99.1875423	0.6809411	01:28.2

Both measured and calculated currents show excellent agreement with certificate values; the calculated current is evaluated from the shunt voltage and resistance respectively. Figure 7 shows the relationship between Certificate Current ($I_{Certificate}$) and Measured Current ($I_{Measured}$). A trend line is fitted to the data points indicates a linear relationship between $I_{Certificate}$ and $I_{Measured}$. The slope of the line is approximately 1, suggesting that the measured current is very close to the certificate current. The intercept is very small ($-5\ x\ 10^{-05}$), which is effectively zero for practical purposes. Coefficient of Determination (R^2) is reported as 1, a perfect fit between the trend line and the data points, this suggests that the measured current values are highly correlated with the certificate current values, with no unexplained variance. The small deviations from the trend line suggest high precision in the measurements. The differences between $I_{Certificate}$ $I_{Calculated}$ and $I_{Measured}$ are minimal as shown in figure 8 and 9, there are no significant outliers in the data. All points lie close to the trend line; the scatter plot provides strong evidence that the measured current values are highly consistent with the certified current values.

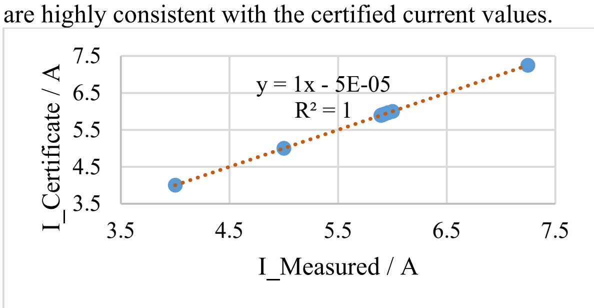

Fig 7. Rrelationship between Certificate Current ($I_{Certificate}$) and Measured Current ($I_{Measured}$)

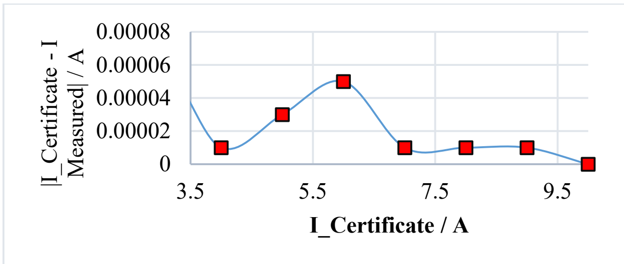

Fig 8. Rrelationship between $|I_{Certificate} - I_{Measured}|$ *and ($I_{Certificate}$)*

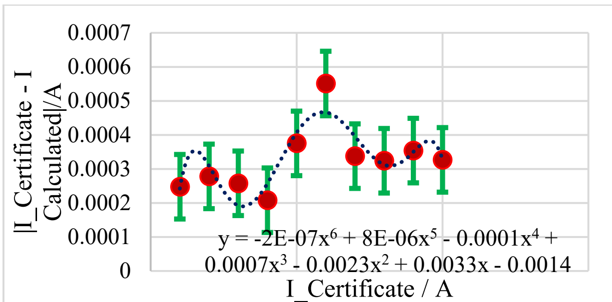

Fig 9. Rrelationship between $|I_{Certificate} - I_{Calculated}|$ *and ($I_{Certificate}$)*

Figure 10 shows the relationship between % PCS (Percentage of precision Current Source) and % Power supply (Percentage of Power Supply) The equation of the trend line indicates a negative linear relationship between % Power supply and % PCS, As % Power supply increases, % PCS decrease. R^2 value of 0.9247 suggests that approximately 92.47% of the variability in % PCS can be explained by the variability in % Power supply. This indicates a strong correlation between the two variables. The data points are clustered around the trend line, indicating that the linear model fits the data well and there are no significant outliers, as all points follow the general trend. The precise measurements and consistent trend suggest that the relationship is robust and reliable.

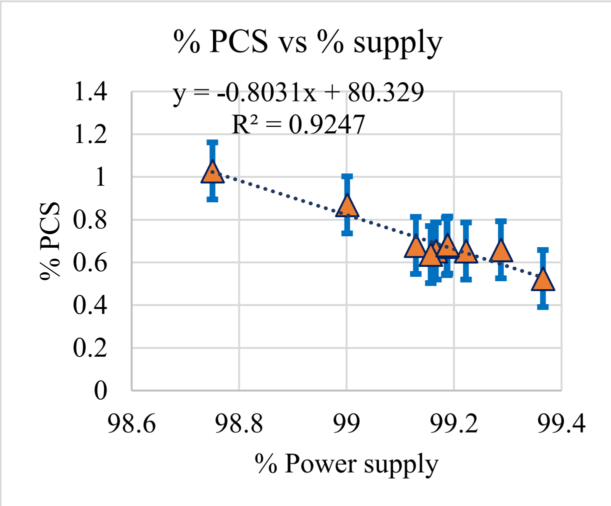

Fig 10. Rrelationship between % Power supply and %PCS

CONCLUSION

The integration of LabVIEW and Python-based AI has successfully transformed the photometry laboratory into a smart, efficient, and reliable testing environment. By automating manual processes and incorporating intelligent analysis capabilities, the system significantly enhances both the accuracy and efficiency of photometric testing. Furthermore, it introduces adaptive and predictive methodologies, enabling more advanced and dynamic testing scenarios. This approach demonstrates the potential of combining industrial automation tools with machine learning to revolutionize traditional optical testing environments, establishing new benchmarks for quality assurance in lighting technologies. Future work will focus on further expanding the AI's capabilities, including the implementation of real-time feedback control systems. Additionally, efforts will explore the application of this framework in other domains, such as radiometry and colorimetry, to broaden its impact and utility across various fields.

REFERENCES

1. The measurement of absolute luminous intensity distributions, CIE Publication, Vol. 70, 1987.
2. The Basis of Physical Photometry, CIE Publication, Vol. 18, 2019.
3. Methods of Characterizing Illuminance Meters and Luminance Meters, CIE Publication, Vol. 69, 1987.
4. The measurement of luminous flux, CIE Publication, Vol. 84, 1989.
5. CASIMER DECUSATIS, Handbook of Applied Photometry, Woodbury, N.Y., AIP Press 1998.
6. RASTELLO M.L., MIRALDI E., PISONI P., J. Appl. Opt. 35 (1996), 4385.
7. Python Software Foundation, *Python*.
8. NumPy Developers, *NumPy*.
9. SciPy Developers, *SciPy*.
10. Pandas Development Team, *Pandas*.
11. Matplotlib Development Team, *Matplotlib*.
12. Seaborn Development Team, *Seaborn*.
13. Python Software Foundation, *Python 3 Reference Manual* . Scotts Valley, CA: CreateSpace Independent Publishing Platform, 2009. ISBN: 978-1-4414-1269-0.
14. T. E. Oliphant, "Python for Scientific Computing," *Computing in Science & Engineering* , vol. 9, no. 3, pp. 10-20, 2007. DOI: 10.1109/MCSE.2007.58.
15. W. McKinney, Python for Data Analysis: Data Wrangling with Pandas, NumPy, and IPython. Sebastopol, CA: O'Reilly Media, 2010.
16. Scikit-learn Developers, *Decision Trees in Scikit-learn*.
17. J. R. Quinlan, "Induction of Decision Trees," *Machine Learning*, vol. 1, no. 1, pp. 81-106, 1986, doi: 10.1007/BF00116251.
18. T. M. Mitchell, *Machine Learning*. New York, NY, USA: McGraw-Hill, 1997.
19. C. M. Bishop, *Pattern Recognition and Machine Learning* . New York, NY, USA: Springer, 2006.
20. S. Russell and P. Norvig, *Artificial Intelligence: A Modern Approach* , 3rd ed. Upper Saddle River, NJ, USA: Pearson Education, 2010.
21. L. Breiman, "Statistical Modeling: The Two Cultures," *Statistical Science* , vol. 16, no. 3, pp. 199-231, 2001, doi: 10.1214/ss/1009213726.
22. V. N. Vapnik, The Nature of Statistical Learning Theory . New York, NY, USA: Springer, 1995.